Paper
Int'l J. of Aeronautical & Space Sci. 17(1), 37–44 (2016)
DOI: http://dx.doi.org/10.5139/IJASS.2016.17.1.37

IJASS
International Journal of Aeronautical and Space Sciences

Multiplexed Hard-Polymer-Clad Fiber Temperature Sensor Using An Optical Time-Domain Reflectometer

Jung-Ryul Lee*

Department of Aerospace Engineering, Korea Advanced Institute of Science and Technology, 291 Daehak-ro,Yuseong-gu, Daejeon 34141, Republic of Korea

Hyeng-Cheol Kim**

Kyeong In Tech Co., Ltd, 15, Paryong-ro 359 Beon-gil, Uichang-gu,Changwon-si, Gyeonsangnam-do 51354, Republic of Korea

Abstract

Optical fiber temperature sensing systems have incomparable advantages over traditional electrical-cable-based monitoring systems. However, the fiber optic interrogators and sensors have often been rejected as a temperature monitoring technology in real-world industrial applications because of high cost and over-specification. This study proposes a multiplexed fiber optic temperature monitoring sensor system using an economical Optical Time-Domain Reflectometer (OTDR) and Hard-Polymer-Clad Fiber (HPCF). HPCF is a special optical fiber in which a hard polymer cladding made of fluoroacrylate acts as a protective coating for an inner silica core. An OTDR is an optical loss measurement system that provides optical loss and event distance measurement in real time. A temperature sensor array with the five sensor nodes at 10-m interval was economically and quickly made by locally stripping HPCF clad through photo-thermal and photo-chemical processes using a continuous/pulse hybrid-mode laser. The exposed cores created backscattering signals in the OTDR attenuation trace. It was demonstrated that the backscattering peaks were independently sensitive to temperature variation. Since the 1.5-mm-long exposed core showed a 5-m-wide backscattering peak, the OTDR with a spatial resolution of 40 mm allows for making a sensor node at every 5 m for independent multiplexing. The performance of the sensor node included an operating range of up to 120°C, a resolution of 0.59 °C, and a temperature sensitivity of -0.00967 dB/°C. Temperature monitoring errors in the environment tests stood at 0.76 °C and 0.36 °C under the temperature variation of the unstrapped fiber region and the vibration of the sensor node. The small sensitivities to the environment and the economic feasibility of the highly multiplexed HPCF temperature monitoring sensor system will be important advantages for use as system-integrated temperature sensors.

Key words: Smart structure, Hard-Polymer-Clad Fiber, Optical Time Domain Reflectometer, Laser clad stripping method

1. Introduction

With the recent development of optical networks, low-cost fiber-optic components have become available. As a result, it has been possible to develop cost-effective fiber-optic sensors for various sensing applications [1]. Fiber-optic sensors offer many benefits over conventional electrical sensors. Most important is their immunity to corrosion and electromagnetic interference, which enables applications under harsh environmental conditions. Fiber-optic sensors have small size, good flexibility, and light weight, and they can be integrated easily into structures, where fiber optics can be used to implement smart structures. They are indispensable for achieving high-speed, large-capacity communication systems [2-4]. The monitoring of physical, chemical, and biological parameters in situ is of great importance for process control in manufacturing industries, for the protection of ecosystems, and for the prevention of global warming. Temperature is

* Professor, Corresponding author: leejrr@kaist.ac.kr
** Staff of Kyeng In Tech Co., Ltd,

Received: July 15, 2015 Revised: January 11, 2016 Accepted: February 24, 2016

http://ijass.org pISSN: 2093-274x eISSN: 2093-2480

one of the most important parameters in these applications [5]. A number of fiber optic methods have been used, and some have been commercialized for industrial temperature measurements [6]. Optical fiber temperature sensors are key devices with a wide range of applications in numerous areas such as aerospace, high-power transformers, buildings, nuclear plants, chemical plants, fire alarm systems for coal mines, and temperature detection for underground power cables. At present, the FBG sensor is popular because of its multiplexing capabilities. However, FBG sensors have temperature-strain cross sensitivity, and the grating writing process is complex, and the photosensitive single-mode fiber is quite expensive [7-12].

A wide range of techniques and approaches have been presented for measuring a very wide set of measurands for a wide range of application sectors [13]. A distributed optical fiber temperature sensing system has incomparable advantages over a traditional monitoring system, whether in the sensing or in the system performance [14]. Periodic or continuous monitoring of structures establishes better maintenance schedules, determines structural health and subsequent safety ratings, verifies load ratings of novel structures and materials, provides fatigue damage information, and improves life-cycle costs. Distributed sensors have been proposed for a number of measurands and have been realized at least at the prototype level to a small extent commercially, but the only real significant success has been the distributed temperature sensor (DTS) [15]. Distributed sensors are most suitable for large structural applications, since all the segments of an optical fiber act as sensors, which allow the perturbations within various segments of the structure to be sensed [16].

Three main types of scattering are known to occur in these sensors: Rayleigh scattering at the original wavelength, Brillouin scattering at a wavelength shifted by about 20 nm, and Raman scattering at a wavelength shifted by about 50 nm [3]. Using Raman scattering, it is possible to obtain distributed temperature measurements over lengths of typically a few kilometers. In contrast to Brillouin scattering, no strain measurement is possible. The Raman scattering produces two broadband components at higher and lower frequencies than the exciting pump wave. Measuring the intensity ratio between these bands, which are called the Stokes and anti-Stokes emissions, it is possible to calculate the temperature at any given point along the fiber line. The Raman backscattering intensity depends on temperature and can be used as a measure for the temperature along the fiber. The Raman backscattered light has two components above and below the incident light: the Raman Stokes and Raman Anti-Stokes peak, as shown in Fig. 1. The backscattered light is spread across a range of wavelengths. Some of these wavelengths are affected by temperature changes, while others are less affected. Using a very accurate detector, the difference in the signal strength is measured, and the temperature is derived from these measurement results. Raman systems are available commercially from York and have been used in different structural monitoring applications [15].

Hard-polymer-clad fiber (HPCF) is one type of optical fiber that has emerged over the last few decades as an option for many optical applications. The HPCF structure is generally a silica core with a clad of thin, hard polymer material and an outer jacket. HPCF is less expensive than all-silica fiber constructions, and offers benefits of high strength, lower static fatigue, less strain at the core-clad interface, high core-to-clad ratios, and lighter weights [17]. HPCF also has merits over plastic optical fiber (POF) in terms of long-distance communication and thermal and mechanical robustness [18].

We propose an economical multiplexed fiber optic temperature monitoring system. The laser clad stripping method is used to elaborate multiple sensor nodes quickly in an HPCF line. The single sensor node length, i.e. the clad removal length, is controlled by adjusting the laser beam diameter, power, and energy [19]. An optical time-domain reflectometer (OTDR) is connected to the HPCF sensor array to test the responses of the multiplexed sensor nodes and normal fiber zones to the changes in temperature and vibration, and to configure a multiplexed HPCF temperature monitoring sensor system by demonstrating the independent temperature sensing capability of each node.

2. Sensing Principle

2.1 Optical time domain reflectometer

The OTDR technique has been a standard tool to investigate broken and damaged locations of optical fibers, and to measure their optical properties. Conventional fiber optic sensors, for example, fiber Bragg gratings (FBG) and

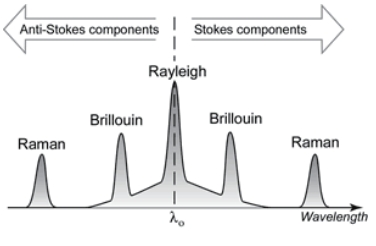

Fig. 1. Raman scattering spectrum [15].

their sensing systems are still too expensive to be accepted in many real-world applications, and too complex to isolate pure temperature measurements because of their multi-measurand sensitivity. Alternatively, OTDR is very cost effective compared to FBG interrogation systems and can easily measure optical loss and its location in real time. An OTDR injects a series of optical pulses into a test fiber and measures the optical intensity of the light scattered (Rayleigh backscatter) or reflected back from the event along the fiber. When a short pulsed light is launched in one end of a sensing fiber, this pulsed light travels through the fiber. This light is scattered everywhere and partially guided back to the launching end. The scattering lights are categorized into three wavelength bands: Rayleigh, Brillouin, and Raman scatterings [20]. Rayleigh backscattering is a linear process. At any point along the fiber, the magnitude of the backscattered optical power is linearly proportional to the optical power at that location. Due to the effect of fiber loss, both the transmitted and the backscattered powers are gradually attenuated along the fiber. The measurement of the time-dependent waveform of the backscattered power at the fiber input terminal provides the information about the loss distribution along the fiber. This information can be used to precisely calculate the attenuation coefficient [21]. A commercial portable OTDR (JDSU MTS-6000 OTDR with a multimode module) with a wavelength of 850 nm and a pulse duration of 10 ns was used to verify the response of the sensor nodes to temperature.

2.2 Temperature sensing principle of clad-removed optical fiber

Figure 2 shows an index profile of the step-index HPCF (BFL37-200, Thorlabs). The fiber used was a multimode HPCF with a numerical aperture (NA) of 0.37, a core diameter of 200 μm, and a cladding diameter of 230 μm, where bare HPCFs without the jacket were used.

Light is guided into the silica core. The fraction of scattered light that travels back toward the input end is described by equation (1) [22]

$$f \sim \frac{(n_1^2 - n_2^2)}{n_1^2} \tag{1}$$

where n_1 and n_2 are the core and clad refractive indices, respectively, and n_3 is that of air, as shown in Fig. 2. In an HPCF, the equation above holds true. When the clad is removed, i.e. $n_2 = n_3 = 1$, the fraction of scattered light (f) at the removed clad part locally increases, and thus, a backscattering peak is observed in the OTDR. If the core temperature increases, the core density decreases, and thus, the core refractive index decreases as well, but the air refractive index (n_3) is barely changed. Therefore, the fraction of the scattered light (f) is decreased, and a lowered backscattering peak is observed in the OTDR. Since a sensor node that is sensitive to the temperature variation is created by removing the clad layer from the optical fiber, dense sensor nodes for quasi-distributed sensing can be fabricated economically.

3. HPCF Temperature Sensor Node Fabrication

Mechanical, chemical, and laser stripping methods are used to remove the clad of polymer-clad fibers. In this study, a continuous-wave-mode/pulsed-mode switchable hybrid diode-pumped solid-state laser with a wavelength of 1064 nm was used to strip the clad off the HPCF, exposing the inner silica core to the external environment [21]. The laser stripping method enabled the control of the removal length easily by considering the beam diameter using equation (2) [17]:

$$B = (I + D)\theta \tag{2}$$

where B is the beam diameter in millimeters, I is the distance from the laser root to the laser head in millimeters, D is the distance in millimeters from the laser head to the HPCF, and θ is the beam divergence angle in radians [15]. The parameters related to the hybrid laser are I = 437.5 mm and θ = 1.6 mrad and the wavelength is 1064 nm. The same setup, energy in the pulsed mode (0.15 J/cm^2 with a 20-Hz pulse-repetition frequency), and power (200 W/cm^2) in the CW mode for the hard polymer clad stripping in Ref. 19 has been used. Varying the separation distance (D = 187.5 mm, 656.5 mm and 812.5 mm) according to equation (2) for the

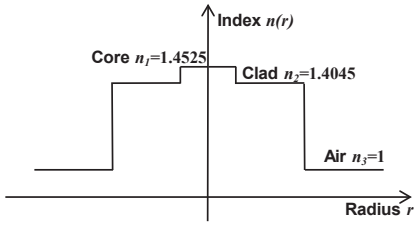

Fig. 2. Refractive index distribution of the hard polymer clad fiber (HPCF).

Table 1. Exposure time of laser beam for the clad removal.

Sensor node length	Pulsed mode	Continuous wave mode
0.75 mm	20 s	3 s
1 mm	20 s	3 s
1.5 mm	25 s	4 s
1.75 mm	35 s	4 s
2 mm	48 s	4 s

beam diameter, 1-mm, 1.75-mm, and 2-mm core lengths were exposed to air to investigate the effect of the exposed core length on the scattering peak signal. The exposure time to remove clads is summarized in Table 1.

4. Experiments & Results

4.1 HPCF sensor node response to different different exposed to node length

The HPCF with a 1.5-mm section of exposed core was first tested under temperature variation by placing it into a thermal chamber and connecting the OTDR to one of the fiber ends, as shown in the experimental setup in Fig. 3(a). The running averaging in signal acquisition was 60 times and the spatial resolution of the OTDR setting was 40 mm. First the back scattering peak induced by removing the clad is observed in Fig. 3(b) and stood at 3.8 dB at the temperature of 20 °C which can be explained by equation (1). The experiment was then conducted by monitoring the peak value of the backscattering signal with respect to the temperature, which ranged from 20 °C to 120 °C. As plotted in Fig. 3(b), the backscattering peak decreased with increasing temperature. As shown in Fig. 3(c), the response to the temperature could be fit to a linear distribution. This implies that the exposed core can be used as a temperature-monitoring sensor node.

Since the backscattering signal is generated from the exposed core, it is imperative to investigate the effect of the exposed core lengths. The 0.75-mm [19], 1-mm, 1.75-mm, and 2-mm sensor nodes were obtained by the proposed methods for laser stripping and control of the core-exposure length. The fabrication time was about 30 s for each sensor node. Those were also placed into the thermal chamber in the same way as in the experiment for the 1.5-mm sensor node, with the temperature varied from 20 °C to 120 °C. As summarized in Fig. 4(a), a longer sensor node generated a higher back scattering peak, and the peak values of the sensor nodes decreased linearly with increasing temperature. In contrast to the 1-mm temperature sensor node, the 1.5-mm and 2-mm temperature sensor nodes with longer exposed core lengths showed linear distributions over the whole temperature range tested. The 1.5-mm sensor node showed a loss rate of -0.01005 dB/°C and R-squared value of linear fit of 0.98207, which was higher than that of the 2-mm sensor

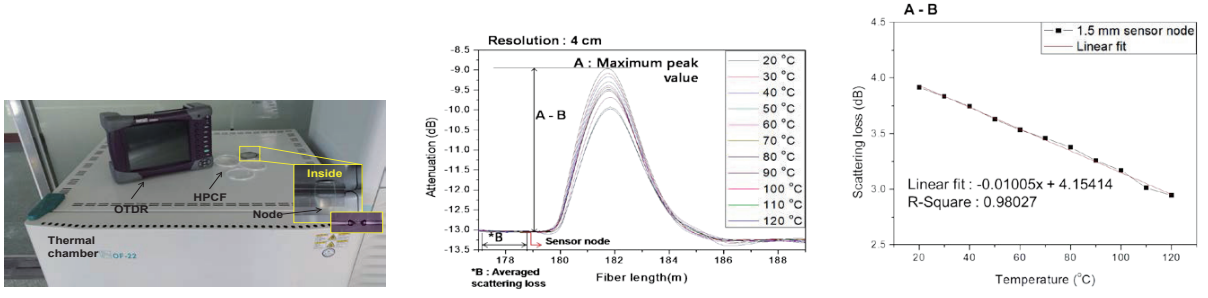

(a) (b) (c)

Fig. 3. (a) HPCF sensor node thermal test setup, (b) 1.5-mm sensor node response at different temperatures, (c) Scattering loss change caused from temperature variation.

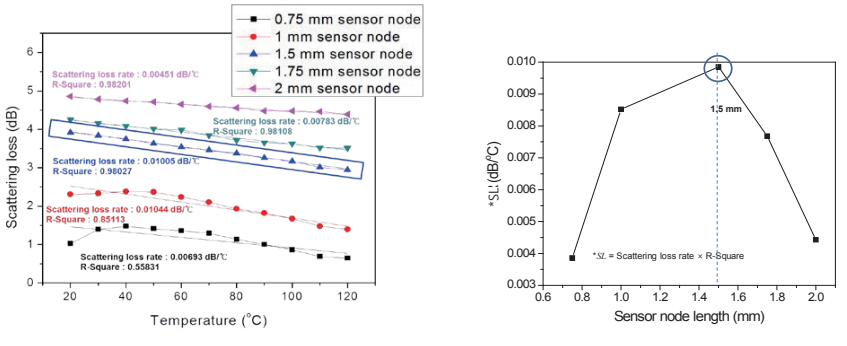

(a) (b)

Fig. 4. (a) Temperature versus the backscattering peak value depending on the sensor node length, (b) Multiplication values of scattering loss rate and R-square depending on the sensor node length.

DOI: http://dx.doi.org/10.5139/IJASS.2016.17.1.37

node. As plotted in Fig. 4(b), the scattering loss rates were multiplied by the R-squared value of the scattering loss linear fits. The scattering loss rate (L) implying the sensitivity and the R-squared value (R^2) related to the measurement linearity was formulated as SL:

$$SL = L \times R^2 \tag{3}$$

The 1.5-mm sensor node out of the sensor node lengths tested showed a maximum SL value and thus the 1.5-mm sensor node was used to develop multiplexed HPCF temperature monitoring sensors.

To investigate the repeatability of the HPCF temperature monitoring sensor, the 1.5-mm sensor node was tested at 40 °C in the thermal chamber. Eight measurements were carried out, and the results are shown in Fig. 5(a). The eight backscattering signals in the OTDR attenuation traces did not show any change. As presented in Fig. 5(b), the measured backscattering peak shows a standard deviation of 0.0058 dB, which corresponds to a temperature-monitoring resolution of 0.59 °C.

To investigate the response of the sensor node against temperature change in the region of the unstripped HPCF, i.e. the original HPCF, an experimental setup was prepared as shown in Fig. 6(a). 10 m of the unstripped HPCF was placed into the thermal chamber, while 14 m of the HPCF with the 1.5-mm sensor node was exposed to room temperature. The total 24-m length of the HPCF was connected to the OTDR. The temperature in the thermal chamber varied from 20 °C to 120 °C. The backscattering signals in the OTDR attenuation trace obtained every 10 °C are shown in Fig. 6(b), and no change is observed. As shown in the analysis in Fig. 6(c), the standard deviation of the backscattering peak depending on the temperature variation of the unstrapped fiber region is 0.00733 dB, which corresponds to a temperature monitoring error of 0.76 °C.

4.2 HPCF sensor node response to environmental vibration

To investigate the response of the 1.5-mm HPCF sensor node to environmental vibration, an experimental setup was

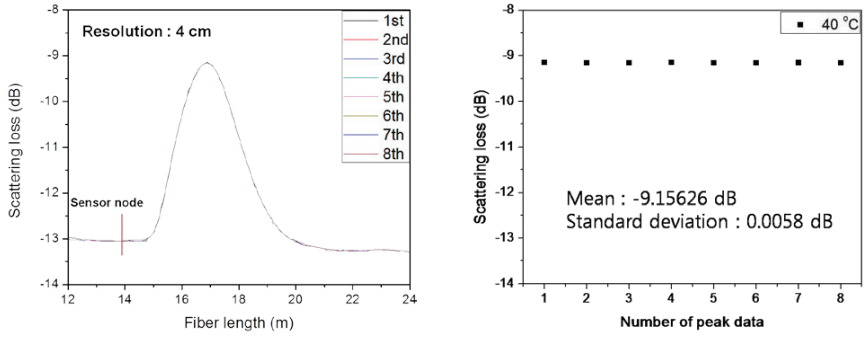

(a) (b)

Fig. 5. (a) Responses of the 1.5-mm sensor node at 40 °C in the eight repetitive measurements, (b) Backscattering peak variation during the repeatability test.

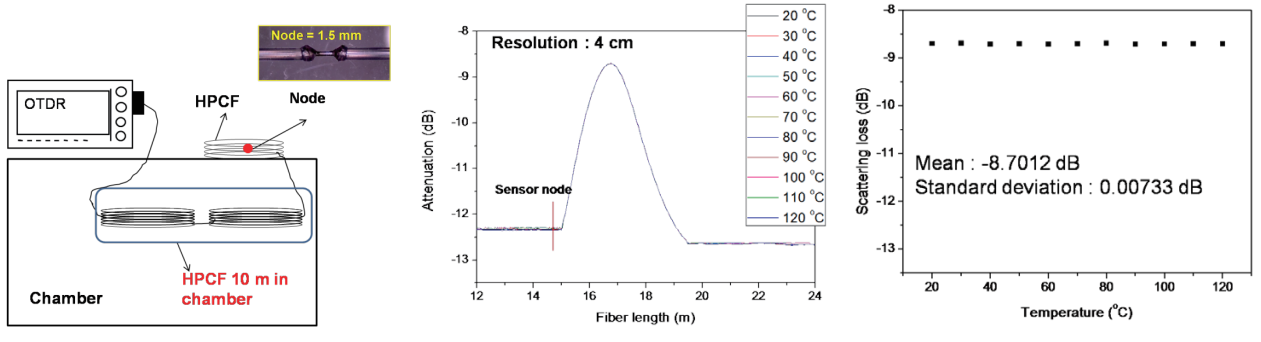

(a) (b) (c)

Fig. 6. (a) Experimental setup to investigate the backscattering signal change caused by temperature variation of the unstripped fiber region, (b) Backscattering signals in OTDR attenuation traces of the 1.5-mm sensor node, (c) variation in the backscattering peak at different temperatures.

prepared as shown in Fig. 7(a). The HPCF was bonded to the shaker, vibration was then applied to the temperature-monitoring sensor node, and OTDR attenuation traces were measured as shown in Fig. 7(b). The sensor node was subjected to 3-Hz sinusoidal excitation between -0.00255g and 0.0034g, 20-Hz sinusoidal excitation between -0.05099g and 0.05099g and random excitation between -0.05099g and 0.05099g among 3 to 20 Hz. As presented in Fig. 7(c), the results did not show any visible change in the OTDR attenuation trace and the standard deviation of the backscattering peak measured during the vibration application was 0.00345 dB, which corresponds to a temperature monitoring error of 0.36 °C. Therefore, the proposed temperature sensor node obtained by removing the clad of the HPCF is insensitive to the vibration. This characteristic is an important merit for use as a temperature-monitoring sensor to be built into structures.

4.3 Multiplexed temperature sensor nodes

The most important advantage of the proposed system is the capability of multiplexed temperature monitoring. To confirm the multiplexed temperature sensor response to temperature, five 1.5-mm-long sensor nodes were made in a single HPCF line by the laser stripping method as shown in Fig. 8. Then, the temperature sensor line was connected to the OTDR. Fig. 9 shows the backscattering of five multiplexed sensor nodes comparing 25 °C with 120 °C. According to the linear fit equation of the 1.5-mm sensor node, the scattering loss value is 3.88815 dB at 25 °C and 2.9695 dB at 120 °C. As shown in Fig. 9, all the sensor nodes stood at scattering losses of about 3.88 dB at 25 °C and then about 2.96 dB at 120 °C. As shown in Fig. 10, the 1st to 3rd sensor nodes were exposed to 120 °C, and the 4th and 5th sensor nodes were exposed to 25 °C. As shown in Fig. 10, the scattering losses of the 1st to 3rd sensor nodes were about 2.96 dB, and those of the 4th and 5th sensor nodes were about 3.88 dB, respectively. Consequently, the multiplexing capability of the proposed system was successfully demonstrated by identifying the temperatures at the respective sensor nodes. Since the 1.5-mm-long exposed core generated a 5-m-wide

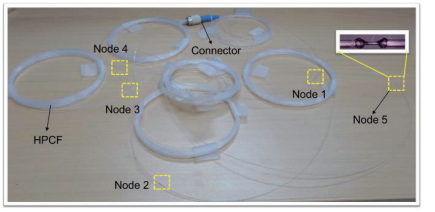

Fig. 8. Developed multiplexed HPCF temperature sensor array.

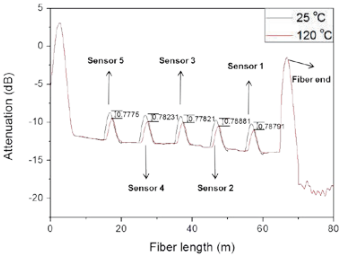

Fig. 9. Attenuation trace change in the five multiplexed sensor nodes exposed to a temperature of 120°C.

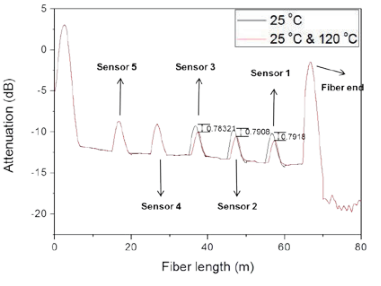

Fig. 10. Attenuation trace change for the case of the 1st to 3rd sensor nodes exposed to a temperature of 120°C and of the 4th and 5th sensor nodes exposed to a temperature of 25°C.

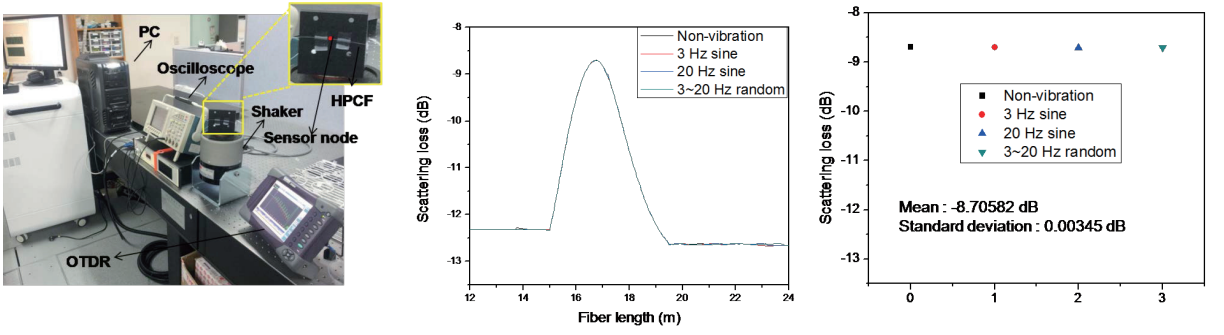

(a) (b) (c)

Fig. 7. (a) Vibration test setup, (b) Responses of the 1.5-mm temperature sensor node to vibration (c) Peak value variation of the back scattering signal caused by vibration.

DOI: http://dx.doi.org/10.5139/IJASS.2016.17.1.37

backscattering signal, the given OTDR allows for a sensor node to be made at every 5 m for independent multiplexing. In fabricating the temperature sensor array in Fig. 8, the core exposure was done for the temperature sensor node at every 10 m, and a backscattering loss of less than 2 dB was used to make the five independent sensor nodes, even though ten sensor nodes could be arrayed. Therefore, at least 35 senor nodes can be arrayed with a single HPCF about 230-m long, and much more sensor nodes can be implemented in a longer HPCF line, which implies various multiplexed temperature monitoring applications can be realized economically by the proposed technique.

5. Conclusion

A multiplexed fiber optic temperature-monitoring sensor system has been proposed using an economical OTDR and HPCF. The sensor nodes were economically and quickly made by locally stripping the clad of HPCF through photothermal and photochemical processes using a CW/Pulse hybrid-mode laser. The core length to be exposed was easily controlled by adjusting the laser beam diameter. Since the fraction of scattered light at the removed clad part locally increased, the backscattering peak happened in the OTDR attenuation trace. When the exposed core temperature increases, the core density decreases, and thus, the core refractive index decreases as well, but the air refractive index (n_3) is barely changed. Therefore, the fraction of the scattered light was decreased, which was observed as the lowered backscattering peak in the OTDR attenuation trace. The sensitivity of the backscattering peak to temperature variation was fitted with a linear distribution. 1.5-mm sensor nodes were selected to develop multiplexed temperature monitoring sensors by measuring the sensitivities and linearity of the respective sensor node lengths.

A temperature sensor array with five sensor nodes at intervals of 10 m was fabricated within 3 min, and the independent temperature monitoring capability of each sensor node was demonstrated. The 1.5-mm-long exposed core showed a 5-m-wide backscattering peak in the 40 mm setting in OTDR resolution. Therefore, it implies that the given OTDR allows for a sensor node to be made at every 5 m for independent multiplexing. The performance of the sensor node included an operating range of up to 120°C, a resolution of 0.59 °C, and a temperature sensitivity of -0.01005 dB/°C. There were temperature monitoring errors in the environment tests at 0.76 °C and 0.36 °C under the temperature variation of the unstrapped fiber region and the vibration of the sensor node. The small sensitivities to the environment and economic feasibility of the highly multiplexed HPCF temperature monitoring sensor system will be important advantages for use as system-integrated temperature sensors in aerospace experiments and systems.

Acknowledgement

This research was supported by the Leading Foreign Research Institute Recruitment Program (2011-0030065) and the Space Core Technology Development Program (2013-042548) through the National Research Foundation of Korea and the research grant (UD130058JD) of the Agency for Defense Development of the Korean government.

References

[1] Marcos, A., R., Valdir, A., S. and Francisco, S., "Side-polished Microstructured Optical Fiber for Temperature Sensor Application", *IEEE Photonics Technology Letters,* Vol. 19, No. 21, 2007, pp. 1738-1740.

[2] Daniel, C.B., Lothar, S., Michael, N.T. and Michael, K., "Structural Monitoring Using Fiber-optic Bragg Grating Sensors", *Structural Health Monitoring*, Vol. 2, No. 2, 2003, pp. 145-152.

[3] Fumio, T., Kazushi, U. and Takeo, K., "Multipoint Temperature Measurement Technology using Optical Fiber", *FUJITSU Sci. Tech.*, Vol. 46, No. 1, 2010, pp. 28-33.

[4] Yoo, W., J., Jang, K., W., Seo, J., K., Moon, J., Han, K., Park, J., Park, B., G. and Lee, B., "Development of a 2-Channel Embedded Infrared Fiber-Optic Temperature Sensor Using Silver Halide Optical Fibers", *Sensors*, Vol. 11, No. 10, 2011, pp. 9549-9559.

[5] Liqiu, M., Ping, L. and Qiying, C., "A Multiplexed Fiber Bragg Grating Sensor for Simultaneous Salinity and Temperature Measurement", *Journal of Applied Physics*, Vol. 103, Issue 5, 2008, pp. 1-7.

[6] Eric, U., "Fiber Optic Sensors; an Introduction for Engineers and Scientists", WILEY-INTERSCIENCE, 2006, pp. 413-419.

[7] Hewa-Gamage, G. and Chu, P., L., "A Multiplexed Point Temperature Fibre Sensor Array using OTDR Technique and TDM Mechanism", *Institute of Electrical and Electronics Engineers*, Vol. 2, 2002, pp. 111-118.

[8] Jianfeng, W., Yongxing, J., Zaixuan, Z., Changyu, S. and Yanqing, Q., "Research of Distributed Optical Fiber Temperature Sensor (DTS) System with Optical Switch", *Institute of Electrical and Electronics Engineers*, Vol. 10, 2010, pp. 1-4.

[9] Moyo, P., Brownjohn, J., Suresh, R. and Tjin, S., "Development of Fiber Bragg Grating Sensors for Monitoring Civil Infrastructure", *Engineering Structures*, Vol. 27, No. 12, 2005, pp. 1828-1834.

[10] Hideaki, I., Hiroshi, Y., Keiji, S. and Akira, M., "Structural Health Monitoring System Using FBG-Based Sensors for a Damage Tolerant Building", *International Workshop on Structural Health Monitoring*, Vol. 1, 2001, pp. 1-10.

[11] Miao, S., Ben, X., Xinyong, D. and Yi, L., "Optical Fiber Strain and Temperature Sensor Based on an In-line Mach-Zehnder Interferometer using Thin-core Fiber", *Optics Communications*, Vol. 285, No. 18, 2012, pp. 3721-3725.

[12] Zhan-Sheng, G., "Strain and Temperature Monitoring of Asymmetric Composite Laminate using FBG Hybrid Sensors", *Structural Health Monitoring*, Vol. 6, No. 3, 2007, pp. 191-197.

[13] Jose, M., Luis, R., Antonio, Q. and Adolfo, C., "Fiber Optic Sensors in Structural Health Monitoring", *Journal of Lightwave Technology*, Vol. 29, No. 4, 2002, pp. 587-608.

[14] Liu, Y., Lei, T., Wei, T., Sun, Z., Wang, C. and Liu, T., "Application of Distributed Optical Fiber Temperature Sensing System based on Raman Scattering in Coal Mine Safety Monitoring", *Institute of Electrical and Electronics Engineers*, Vol. 1, 2012, pp. 1-4.

[15] Jose, M., L., "Handbook of Optical Fibre Sensing Technology", WILEY, 2002, pp. 482-493.

[16] Hong-Nan, L., Dong-Sheng, L. and Gang-Bing, S., "Recent Applications of Fiber Optic Sensors to Health Monitoring in Civil engineering", *Engineering Structures*, Vol. 26, No. 11, 2004, pp. 1647-1657.

[17] Yun, C. Y., Dipesh, D., Lee, J. R., Park, G. and Kwon, I. B., "Design of Multiplexed Fiber Optic Chemical Sensing System using Clad-removable Optical Fibers", *Optics & Laser Technology*, Vol. 44, No. 1, 2012, pp. 269-280.

[18] Kim, D. U., Bae, S. C., Kim, J., Kim, T. Y., Park, C. S. and Oh, K., "Hard Polymer Cladding Fiber (HPCF) Links for High-Speed Short Reach 1 4 Passive Optical Network (PON) Based on All-HPCF Compatible used Taper Power Splitter", *Institute of Electrical and Electronics Engineers Photonics Technology Letters*, Vol. 17, No. 11, 2005, pp. 2355-2357.

[19] Kim, H. C. and Lee, J. R., "A Novel Fiber Optic Temperature Monitoring Sensor using Hard-polymer-clad fiber and Optical Time-domain Reflectometer", *Journal of Intelligent Material Systems and Structures*, Vol. 25, No. 5, 2014, pp. 654-661.

[20] Hwang, D., Yoon, D., Kwon, I., Seo, D. and Chung, Y., "Novel Auto-correction Method in a Fiber-optic distributed-temperature Sensor using Reflected Anti-Stokes Raman Scattering", *Optics Express*, Vol. 18, No. 10, 2010, pp. 9747-9754.

[21] Rongqing, H. and Maurice, O., "Fiber Optic Measurement Techniques", ELSEVIER ACADEMIC PRESS, 2009, pp. 384-385.

[22] Kohich, A., Kiyoshi, N. and Takeshi, I., "Optical Time Domain Reflectometry in a Single-Mode Fiber", *IEEE Journal of Quantum Electronics*, Vol. 17, No. 6, 1981, pp. 862-868.

[23] Kalpakjian, S. and Schmid, S. R., *Manufacturing Processes for Engineering Materials*, Second Ed. Addison-Wesley Publishing Company, New York, USA, 1992.